J Solid State Electrochem (2009) 13:991–997
DOI 10.1007/s10008-008-0683-3

ORIGINAL PAPER

A model for high-surface-area porous Nafion™-bonded cathodes operating in hydrogen–oxygen proton exchange membrane fuel cells (PEMFCs)

A. J. Appleby

Received: 2 August 2008 / Revised: 15 September 2008 / Accepted: 17 September 2008 / Published online: 22 October 2008

Abstract A critical discussion of dioxygen reduction kinetics using the Tafel (for the irreversible cathode process) and the Butler–Volmer (anode process) rate equations has been used to evaluate the accuracy of "standard" modeling interpretations of experimental cell potential current (*E–I*) plots. The potential–current curve for what is believed to be an optimized Nafion™-bonded fuel cell cathode was analyzed. It appears to behave as a well-ordered diffusional system and shows high electrocatalyst utilization based on its electrocatalytic and gas diffusion characteristics. The electrode appears to perform as expected, without any anomalous characteristics showing any lower than expected electrocatalyst utilization. Any improvement in electrode performance, which is certainly desirable, seems to demand an improved diffusional structure, barring any potential (although unlikely) change in electrochemical kinetic characteristics.

Keywords Electrocatalysis · Dioxygen reduction · PEMFCs · Porous electrodes · Electrode models

Introduction

The potential–current curve of acid electrolyte fuel cells, particularly that of the proton exchange membrane fuel cell (PEMFC), consists of an apparently kinetically limited (Tafel) region at low current density, a rather long quasi-linear region centered around the point of minimum voltage–current slope which has been usually interpreted as ohmic, and a gently sloping region over a rather wide range of current density towards a tendency to a limiting current. This is discussed in more detail later. The important point to note is that the rate of change of slope between the Tafel region and the start of the linear region is much greater than that a high current density. As would be expected, the trend to a limiting current is greater at lower electrocatalyst loadings (i.e., with reduced electrocatalytic area), when it occurs at lower current densities, and also at lower reactant partial pressures, particularly at the cathode. It should be also obvious that the highly irreversible cathode potential–current density curve for dioxygen reduction should normally be separated from that of the polarization curve for the hydrogen anode, which is close to reversible for platinum electrocatalyst at all accessible current densities with well-designed electrode structures. For example, Neyerlin et al. [1] have measured anodic exchange currents of 235–600 mA cm^{-2} of platinum area on ultra-low-loading electrodes with this system, corresponding to polarizations of 50 mV at 2.0 A cm^{-2}. However, this separation has not often been attempted in "standard" modeling interpretations of experimental *E–I* plots, although experimental impedance work using a pseudo-reference electrode [2, 3] and theoretical models for individual reaction steps [4] are recent exceptions.

The overall PEMFC cell potential has generally been modeled [5–8] using an expression of the type:

$$E = E_o - b\ln(i/i_o) - E[f(\Delta C)] - iR \quad (1)$$

where E is potential or overall cell voltage, E_o is the theoretical reversible potential, i is the measured current density, i_o is the extrapolated exchange current density, b is the natural logarithm Tafel slope taken from the experimentally

Dedicated to the 85th birthday of John O'M. Bockris.

A. J. Appleby (✉)
Center for Electrochemical Systems and Hydrogen Research,
Texas A&M University,
College Station, TX 77843-3402, USA
e-mail: ajappleby@tamu.edu

accessible region of i, R is an ohmic resistance, and $Ef(\Delta C)$ is an empirically fitted function used to represent depletion of reactants at high current density, in particular at the cathode. For a system with well-defined hydrodynamics, such as the perpendicular current to a rotating disc electrode (RDE) or that to a thin uniform layer of solid electrolyte over an active electrode, $E[f(\Delta C)]$ is readily defined. In general, the measured current density i is given by:

$$i = x(C_o - C_s) = i_d - xC_s = yC_s^z \quad (2)$$

where x is the diffusion rate constant, i.e., D/δ, in which D and δ are the effective values of the diffusion coefficient and the diffusion layer thickness, C_o and C_s are the bulk and electrode surface concentrations of the diffusing reactant whose kinetic reaction order is z, i_d is its diffusion-limiting current, and y is the potential-dependent electrochemical rate constant. Rearranging, we obtain:

$$i_k = yC_o^z = yC_s^z[i_d/(i_d - i)]^z = i[i_d/(i_d - i)]^z \quad (3)$$

where i_k is the kinetic current at the bulk electrolyte concentration at the local potential. The special case of this relationship when $z=1$ has been commonly used to derive i_k to give the kinetic Tafel plot at bulk concentration C_o from the measured i–E data from the diffusion wave at a rotating disc electrode at constant rotation rate in liquid electrolyte media [9].

Using 3, the expression for E (Eq. 1) becomes:

$$E = E_o - b\ln(i/i_o) + zb\ln[1 - (i/i_d)] - iR. \quad (4)$$

If the above diffusional and kinetic reaction order conditions for the system are met, then $-E[f(\Delta C)]$ in Eq. 1 is equal to $+zb\ln[1-(i/i_d)]$. Previous empirical expressions used for $-E[f(\Delta C)]$ in the literature [5–7] are shown (with comments) in Table 1.

If we write $i_k = i_o \exp(\eta/b) = i_o \exp \alpha F\eta/\mathrm{RT}$, where η is overpotential, we obtain the equation for the wave:

$$\eta = b\ln\{(i/i_o)[i_d/(i_d - i)]^z\}. \quad (5)$$

Table 1 Expressions for the empirical $-E[f(\Delta C)]$ term used in recent literature

Reference	Expression for $-E[f(\Delta C)]$	Comments
Eq. 1, here	$+zb\ln[1-(i/i_d)]$	
[5]	$-m\exp(ni)$	m and n are fitted constants
[6, 8]	$+\alpha i^k \ln[1-(i/i_d)]$	α and k (≈3) are fitted constants
[7]	$i-i_{min}$	i_{min} is the minimum value of i showing a deviation from linearity in the central E–i plot region

For $z=1$, the wave is symmetrical, whereas other values of z introduce some asymmetry. This may be seen by differentiation of 3, giving:

$$d\eta/di = -b[i_d + i(z-1)]/[i(i_d - i)]. \quad (6)$$

Thus, the slope increases with increasing i compared with the $z=1$ case for $z>1$ and falls with increasing i compared to the $z=1$ case for $z<1$. In the general case, the minimum slope ($d\eta/di_d$) occurs at $(i/i_d) = (1+z^{0.5})^{-1}$ and is $b(1+z^{0.5})^2$, while the slope at the half-wave potential is $2b(1+z)$.

If the system under study is a complete PEMFC (or other low temperature fuel cell), then the $d\eta/di$ relationship for the anode, as well as the ohmic resistance, must be added to give the overall $d\eta/di$ relationship. The hydrogen oxidation anode reaction on effective practical electrocatalysts (high-surface-area platinum) is quite reversible [1] at accessible current densities and is not diffusion-limited, and its $d\eta/di$ slope is (by expansion of the exponentials in the rate equations for the anodic and cathodic reactions) equal to $(1/i_o)[\mathrm{RT}/(\alpha_a + \alpha_c)F]$ where α_a, α_c are the anodic and cathodic hydrogen electrode transfer coefficients, respectively. If the overall hydrogen electrode process consist of successive electron steps, i.e., the Heyrovsky and Volmer reactions $H_2 \rightarrow H_{ads} + H^+ + e^-$; $H_{ads} \rightarrow H^+ + e^-$; it is readily shown that $(\alpha_a+\alpha_c)$ will be 2 provided that the rate-determining step (rds) is continuous throughout the near-equilibrium potential range at all adsorbed reactant coverages. However, if the chemical Tafel (combination) reaction $2H_{ads} \rightarrow H_2$ is followed by the Volmer reaction, as is generally accepted on high-surface-area platinum in acid media [10, 11], this will make $\alpha_a+\alpha_c=1.0$.

At PEMFC operating temperatures (e.g., 70 °C, 343 K), RT/F is about 29.5 mV. For the hydrogen electrode reaction, i_o per geometrical unit area of porous electrode is very large, so the anode reaction impedance (which for a complete cell must be added to the dominant cathode kinetic impedance) is quite small. Thus, the cell impedance at the half-wave potential of a complete optimized PEMFC will be $4\mathrm{RT}/\alpha F$ for $z=1$, plus any iR losses, where α is the local irreversible *cathodic* transfer coefficient at that potential.

rds for dioxygen reduction

It seems to be generally accepted that dioxygen reduction in the oxygen reduction reaction (ORR) is kinetically of the first order at constant reference potential on the most effective electrocatalyst, platinum, in aqueous media. This contrasts to the analysis of Kuhn et al. [4] in which it is assumed that dissociative adsorption of dioxygen occurs as a preliminary rapid step before initial rate-determining charge transfer, which would correspond to a reaction order of 0.5. The most commonly cited rds at low current density,

where the Tafel slope is about RT/*F*, is that proposed by Damjanovic and Brusic [12]. The Occam's razor principle generally applies to any electrochemical rds or indeed any chemical rds. This means that it should be as simple as possible, involving the minimum number of molecules or ions as reactants and products and involving a maximum of only one electron. The proposed rds for the Damjanovic–Brusic mechanism in acid media is:

$$O_2 + H^+ + e^- \rightarrow HO - O_{ads} \quad (A)$$

in which the O_2 reactant is either in a position close to the adsorption site, or merely physisorbed, prior to reaction. It is postulated that the HO–O– radical is catalytically chemisorbed to a platinum site via its free oxygen atom. Whether protons are involved in the rds as given above is disputed, since some researchers postulate an rds with a $O - O^{\bullet}$ – product, where $^{\bullet}$ refers to a free electron [13–15]. In principle, this may be determined by the effect of pH on the reaction rate. This is discussed in more detail below.

Whether O_2 is associated with a single site or pair of sites, or physisorbed either vertically to a single site, or horizontally to one or to a pair of sites, may well determine the course of the reaction to its ultimate products. Association with a pair of sites might be propitious for bond dissociation to eventually give two side-by-side $–OH_{ads}$ products, which should then result in rapid production of product H_2O, whereas single-site adsorption associated with unavailable neighboring sites may be expected to result in two-electron reduction to H_2O_2, which would itself require migration to paired sites where bond dissociation might occur.

Accepting for the moment reaction (A) as the rds at low current density, the ln reaction rate will be given by:

$$\ln i = \ln[O_2] + \ln[H^+] + \ln k_A + x\ln(1-\theta_T) - (1-\beta)\Delta G_{(ads)HO_2}/RT - \beta FE/RT \quad (7)$$

where the square brackets are reactant activities, k_A is the rate constant at E and $\Delta G_{(ads)HO_2} = 0$, and $(1-\beta))\Delta G_{(ads)HO_2}$ is the free energy of adsorption of $HO_{2(ads)}$ at E=0 multiplied by the appropriate Brønsted coefficient for a product, and x is the reaction order for reaction sites [13–15] whose coverage is $(1-\theta_T)$, where θ_T is the total coverage of all adsorbed species.

However, in the potential range where the RT/*F* slope is observed, bulk polycrystalline Pt surfaces carry a low-to-medium coverage of species derived from water oxidation:

$$H_2O \rightarrow OH_{(ads)} + H^+ + e^- (\text{starting at } 0.75 - 0.8\,\text{V vs. HE}) \quad (B)$$

where HE is the hydrogen electrode potential in the same medium and

$$OH_{(ads)} \rightarrow O_{(ads)} + H^+ + e^- (\text{at higher potentials vs. HE}) \quad (C)$$

As cyclic voltammetry shows, the lower coverage adsorbate (B) is reversible, whereas after a coverage of 0.33 on a Pt(111) surface, adsorbates start to occupy neighboring sites. This starts the formation of island phases, which is followed by essentially irreversible formation of $O_{(ads)}$ islands, which reduce in a slow process characterized by a rather Langmuirian peak (i.e., distinctive of a single chemical phase) centered at about 0.8 V vs. HE [16]. On polycrystalline and Pt(hkl) surfaces, dioxygen reduction occurs in an accessible potential and current density range where (B) under reversible conditions is important. This adsorption is associated with a Frumkin isotherm in which the free energy of adsorption of $OH_{(ads)}$ becomes more positive, essentially linearly, with its coverage $\theta_{(OH)}$ in the medium coverage range due to sideways repulsions. The Frumkin isotherm for adsorption of $OH_{(ads)}$ in reaction (B) is:

$$\ln[\theta/(1-\theta_T)] = \ln[H_2O] - \ln[H^+] - \Delta G_{(ads)OH}/RT - q\theta_T/RT + FE/RT \quad (8)$$

where $\Delta G_{(ads)OH}$ is the free energy of adsorption at low coverage and E=0, and q is the change in free energy of adsorption on going from low to high coverage. The standard state for θ is 0.5, when $[\Delta G_{(ads)OH}/RT - 0.5q/RT + FE/RT] = 0$. If we postulate that such a reduction in free energy will affect all similar species on the electrode surface, then $-(1-\beta)\Delta G_{(ads)HO_2}/RT$ may be written $(1-\beta)\times(\Delta G_{(ads,0)HO_2}/RT - q\theta/RT)$ where the $\Delta G_{(ads,0)}$ value is that at low coverage. We then postulate that the coverage of $HO_{2(ads)}$ is small compared with that of $OH_{(ads)}$, which is consistent with the bond strengths in $H–O_2H$ and H–OH, so the θ term in 8 is replaced by θ_T.

It may be argued that the above approach is an empirical hypothesis, since it does not account for the oriented water dipoles in the compact double layer and the competition between their adsorption and that of reaction intermediates and $OH_{(ads)}$, which has been modeled by Franco et al. [2, 3]. A reaction intermediate displaces one or more water dipoles from the platinum surface, and a water dipole is converted into $OH_{(ads)}$ with the loss of an electron to the metal and of a proton to the bulk electrolyte. Thus, an electronic charge crosses the entire double layer, as it does when, e.g., an electron from the metal and a proton from the electrolyte are simultaneously transferred to adsorbed dioxygen, so in both cases, the whole of the inner layer potential difference acts on the electrochemical activation energy.[1] The effect of the competition between water dipole

[1] In contrast, if only an electron is transferred from the metal to e.g., $O_{2(ads)}$, with no simultaneous proton from the solution, the transferred charge may see a potential gradient less than that between the metal and electrolyte, resulting in a higher Tafel slope. This would be expected to be replaced by a dominant reaction involving complete charge transfer across the interface.

adsorption and $OH_{(ads)}$ may probably be neglected, since the chemical free energy of the latter is probably not only significantly higher than that of the electrostatic adsorption of a water dipole, but the experimental $OH_{(ads)}$ coverages recorded by cyclic voltammetry or charging curves already reflect the difference in free energy of adsorption between this species and water. The same may be true for $HO_{2(ads)}$ adsorption, while the corresponding situation for $O_{2(ads)}$ vs. that of water dipoles is more open to question. Franco et al. [2, 3] consider that neglecting the effect of water dipole adsorption on $(1-\theta_T)$ might be important, which may require further consideration. This is outside the scope of this paper. However, these authors neglect the well-established coverage dependence of the free energy of adsorption of $OH_{(ads)}$ [12–15] and the working hypothesis that the same coverage dependence applies to all chemically adsorbed species [12–15]. This may explain why their calculated coverages are higher than experimental data.

The usual approach in the literature has been to neglect the ln coverage terms [12] in Eqs. 7 and 8, which also means neglecting the effect of x. If we do this at constant water activity, 8 becomes:

$$-q\theta_T/RT = \ln[H^+] + \Delta G_{(ads)OH}/RT - FV/RT. \quad (9)$$

Substituting this in 7 gives:

$$\begin{aligned} \text{lni} = {} & \ln[O_2] + (2-\beta)\ln[H^+]\ln k_A \\ & - (1-\beta)\Delta G_{(ads)HO_2}/RT + (1-\beta)\Delta G_{(ads)OH}/RT \\ & - FE/RT \end{aligned} \quad (10)$$

since $E = \eta + (RT/F)\ln[H^+]$, the reaction order for protons is $(1-\beta)$ at constant η at constant potential vs. HE. However, Eq. 10 is only exact at θ=0.5 and x=1. If the pre-exponential for θ were retained in Eqs. 7 and 8, the reaction order for protons and the Tafel slope would differ from these values. A complete treatment [17] including all pre-exponential θ_T terms and postulated x values of 1 and 2 for β=0.5 gives the exact values of $(F/RT)(\partial \text{lni}/\partial\eta)$ and $\{\partial \text{lni}/\partial \ln[H^+]\}_\eta$ shown in Table 2, which vary significantly as a function of θ_T.

A θ_T value of 0.1 at 0.8 V vs. HE appears to be reasonable for both bulk platinum [12] and platinum nanocrystals rather than the higher value reported for well-ordered Pt(111), which shows different adsorption characteristics for both OH_{ads} and particularly for anions [14]. Using a q/RT value of 9.9 at 333 K estimated from the value for the Pt(111) face in 0.1 M $HClO_4$ from [14], these coverages would correspond to those at 0.76, 0.80, 0.85, 0.90, 0.94, and 0.98 V vs. HE, respectively. The maximum value of θ to which this analysis might probably apply would, however, be 1/3 on the Pt(111) face, corresponding to 0.91 V in this data fit, since this is the maximum value for all $OH_{(ads)}$ adsorbate species that are separated by an unoccupied site. At this coverage, each pair of empty sites is in contact with four $OH_{(ads)}$ sites, two end-on and two sideways. This environment would not be propitious for rate-determining formation, followed by rapid dissociation, of $O_2H_{(ads)}$. At a coverage of 1/4 (at about 0.88 V vs. HE), pairs of sites have two nearest-neighbor $OH_{(ads)}$. At a coverage of 1/6 (at about 0.84 V vs. HE), some pairs of sites are in contact with only one $OH_{(ads)}$, which should be favorable for a rapid dissociation step following the first electron transfer rds.

Table 2 Calculated values of $(F/RT)(\partial \text{lni}/\partial\eta)$ and $\{\partial \text{lni}/\partial \ln[H^+]\}_\eta$ with β=0.5 as a function of total chemisorbed species coverage, θ_T, as a function of the reaction order x for vacant surface sites (x=1, 2)

θ_T: x=1; x=2	$(F/RT)(\partial \text{lni}/\partial\eta)$	$\{\partial \text{lni}/\partial \ln[H^+]\}_\eta$
0.05	0.69; 0.73	0.19; 0.23
0.1	0.79; 0.84	0.29; 0.34
0.2	0.88; 0.96	0.38; 0.46
0.3	0.94; 1.03	0.44; 0.53
0.4	0.97; 1.09	0.47; 0.59
0.5	1.00; 1.14	0.50; 0.64

Another reason for accepting a process such as (A) with a single adsorption bond formed in the rate-determining step is the relationship between the experimental Arrhenius activation energy at constant η and the estimated $\Delta\Delta\eta_{(ads)}$ of oxygenated species on a series of Group VIII noble metals in concentrated phosphoric acid. The corresponding slope is close to 0.5 [18], which corresponds to the expectations of Eq. 7 at low coverage. This old work requires a reevaluation in a dilute non-adsorbing acid medium, e.g., $HClO_4$ or CF_3SO_3H.

The approximately RT/F Tafel slope observed above approximately 0.8 V HE might be interpreted as a chemical rds taking place under low-coverage Langmuir adsorption conditions following a rapid one-electron step, e.g., step A followed by:

$$HO - O_{(ads)} \rightarrow OH_{(ads)} + O_{(ads)} \quad (D)$$

or even [2, 3, 19] by the reaction:

$$HO - O_{(ads)} + H_2O \rightarrow 3OH_{(ads)}. \quad (E)$$

However, these may be eliminated since at least one of the products of these steps is chemically equivalent to the product of reaction (B) and should be affected by $q\theta_T$/RT under Frumkin isotherm conditions, as has been discussed above. As [17] indicates, the result will be $(F/RT)(\partial \text{lni}/\partial\eta)$ and $\{\partial \text{lni}/\partial \ln[H^+]\}_\eta$ values which do not correspond to the observed kinetics above 0.8 V vs. HE. At a sufficiently low potential below 0.8 V vs. HE, a Tafel slope of RT/βF≈2RT/F will be expected for reaction

(A) under Langmuir (low coverage) conditions, with $\{\partial \ln i/\partial \ln[H^+]\}_E = +1$ and $\{\partial \ln i/\partial \ln[H^+]\}_\eta = 0.5$.

While again these require further experimental confirmation, a fairly convincing case may be made for a Damjanovic–Brusic mechanism for medium coverage of $OH_{(ads)}$ in the medium coverage range down to some potential vs. HE of 0.8 V or somewhat less in non-adsorbing acid media, which will be followed at more negative potentials, by the same rds occurring under low-coverage conditions. On conventional bulk polycrystalline Pt or single-crystal Pt(hkl) electrodes used as RDEs in such media, the potential range which can normally be explored is usually restricted to a range of $V \approx 0.80$–0.95 vs. HE. In porous diffusion electrodes in the PEMFC, a region of from 0.8 to about 0.6 V vs. HE (including IR drop) includes the linear slope region for which kinetic information is generally inaccessible. For the most part, the Tafel slope in this low-coverage region should be $\approx 2RT/F$. Antoine et al. [19] give rather convincing evidence of the applicability of the Damjanovic–Brusic rds [12] to high-surface-area carbon-supported Pt electrocatalysts. The rate-determining step (A) is most likely followed by a second combined proton and electron transfer step[2] involving dissociation to give two $OH_{(ads)}$ on adjacent sites, i.e.,

$$O_2H_{(ads)} + H^+ + e^- \rightarrow OH_{(ads)} + OH_{(ads)}. \quad (F)$$

This will be followed by rapid desorption via the reverse of reaction (B).

From the above discussion, the analyses given in the empirical equations to explain E–i curves for porous PEMFC electrodes [5–8] may be misleading. The pseudo-ohmic linear region in their polarization curves may be partially mass-transport-limited rather than purely ohmic, analogous to a classical first-order polarographic wave for an irreversible process. The dimensionless current equation for a first-order wave under well-defined diffusional conditions (derived from Eq. 3) is:

$$(i/i_d) = (i_k/i_d)/[(i_k/i_d) + 1], \text{i.e., } i = i_k i_d/(i_k + i_d). \quad (11)$$

(i/i_d) is a symmetrical expression centered around $(i/i_d)=0.5$ (at the half-wave potential) where $(i_k/i_d)=1$. With $i_k = i_o \exp -\alpha F\eta/RT$, the general expression for the $d\eta/di$ slope is $(-RT/\alpha F)[i_d/i(i_d - i)]$. The center portion of the slope around the half-wave potential ($0.25 < i/i_d < 0.75$) is rather flat, and at the half-wave potential, the IR-corrected E–i slope should be $(-4RT/\alpha F i_d)$.

A good case may be made that porous PEMFC electrodes containing Nafion™ electrolyte as a binder may be, microscopically, a rather well-defined diffusional system. This is because they consist of catalyst particles joined by Nafion™ bridges, as is illustrated in [8]. These bridges define the limits of three-dimensional gas pores through which oxygen diffuses via the thin bridge to each catalyst particle. Overall, an optimized electrode should be a rather well-defined diffusional system, certainly compared with a fuel cell electrode with liquid electrolyte, whose volume in the pores becomes greater by dilution with water at high current densities. At low current density, it is well known that platinum catalyst utilization is rather high when optimum amounts of Nafion™ ionomer are used with optimized pressing conditions. However, at high current densities, catalyst utilization falls as current density increases. This was attributed by Fischer et al. [20] to the accumulation of liquid water in the open pores, inhibiting oxygen diffusion,[3] which is why empirical equations [5–8] were devised to explain experimental results.

The analysis given above, which determines the local value of α, is rather well borne out by the polarization data for PEMFC anodes and cathodes containing an optimum 33 wt.% Nafion™ (Du Pont de Nemours, Wilmington, DE, USA) in Fig. 1 of Passalacqua et al. [8]. Their anodes and cathodes consisted of 0.1 mg cm^{-2} 20 wt.% platinum on carbon (E-TEK Division of Pemeas GmbH, Somerset, NJ, USA) and had an effective electrochemical surface area as measured by underpotential hydrogen deposition voltammetry of 73 m^2 g^{-1} (73 cm^2 per geometric square centimeter). Current density–cell voltage results were obtained on a fuel cell containing these electrodes and Nafion™ 117 PEM electrolyte operating at 70 °C on hydrogen and air at 2.5 and 3.0 bar absolute humidified to 85 °C and 80 °C, respectively. The anode and cathode gases were constant flow, corresponding to 1.5 and 2.5 times the stoichiometric requirement at 1.0 A cm^{-1}. Resistance data were obtained by current interruption in the 0.2–0.3 A cm^{-2} range using a storage oscilloscope. The result obtained was $0.22 \pm 0.02\ \Omega\ cm^2$.

The first item of interest is that the cell resistance Passalacqua et al. obtained by curve fitting using Eq. 1 was 50% higher than the experimental value determined by current interruption. The second is that the E–i curve for their cell (i.e., the wave) corrected for iR drop determined by the interrupter technique was not symmetrical, as is predicted by Eq. 6 for a wave of the first kinetic order. The change of slope of the corrected plot, which from Eq. 6, should be proportional to b or to $1/\alpha$, where α is the charge transfer coefficient for oxygen reduction. b changes with current density or potential from rapid values at low current

[2] However, the impedance results of Kuhn et al. [2, 3] suggest that a chemical step occurs in the reaction sequence. This may be $O_2H_{(ads)} \rightarrow OH_{(ads)} + O_{(ads)}$, while $O_2H_{(ads)} + H_2O \rightarrow 3OH_{(ads)} + O_{(ads)}$ appears less probable. This requires further evaluation.

[3] Other explanations are offered by Franco et al. [2, 3], at least for long operating times.

density (potential above about 0.8 vs. HE) to lower values below about 0.75 V. This is particularly apparent in the difference in curvature between the sharp change in the low-current density region and in the region approaching the cathode-limiting current (0.862 A cm^{-2}), as estimated from data in [8]. An approximate analysis of these data appears to show that the rate of change of slope at high current density is about half of that at low current density. While one explanation of this effect may be a change of x with potential or current density (Eq. 6), a more likely explanation is a change in α under these conditions, as would be expected from the Damjanovic–Brusic mechanism.

After removal of the experimental iR drop for the electrode in question, $d\eta/di_d$ at the half-wave potential from Fig. 1 of the Passalacqua et al. paper corresponds to α= 0.48, a good value for a first electron transfer rate-determining step under Langmuir adsorption conditions at low coverage. This slope is measured between about 0.8 and 0.7 V vs. HE. At these potentials, the coverage of reversibly adsorbed oxygenated species, i.e., $OH_{(ads)}$, is low.

We use Eq. 7 for the rate of reaction (A), with the Eq. (8) for the $OH_{(ads)}$ adsorption isotherm, including all pre-exponential θ terms, with n=2 to account for reaction (F), with (as above) θ_T normalized to 0.1 at 0.8 V vs. HE, q/RT= 9.9, and i_k normalized to 0.120 A cm^{-2} at 0.8 V vs. HE, calculated using the second part of Eq. 11. This value corresponds to i=0.105 A cm^{-2} under these conditions, with i_d estimated to be 0.862 A cm^{-2} [8]. The resulting calculated $E-\log_{10} i$ plot with β=0.5 is shown in Fig. 1. It has the properties expected: a region of ln Tafel slope of about RT/F

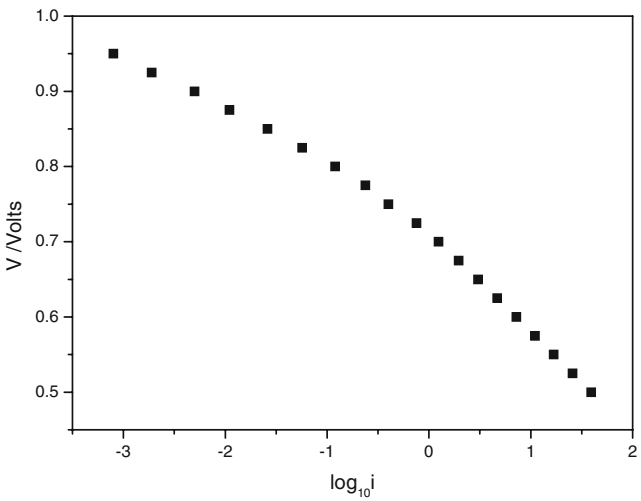

Fig. 1 Modeled Tafel plot for an optimized PEMFC cathode with 0.1 mg cm^{-2} 20 wt.% Pt/C electrode containing 0.33 wt.% Nafion™ binder operating on 3.0 atma air (i.e., 0.63 atma oxygen) at 70 °C [8]. The model uses the rate Eq. 7 with x (reaction order for surface sites)= 2, and the Frumkin isotherm Eq. 8. It assumes q/RT=9.9, β=0.5, and θ=0.1 at V=0.8 V and is normalized to a current density of 0.120 A cm^{-2} at 0.8 V to agree with the result in Fig. 2

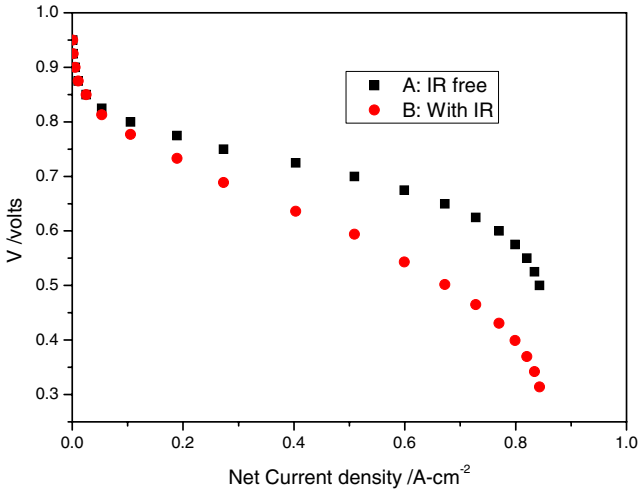

Fig. 2 *Upper plot*: Polarization data for the cathode in Fig. 1 calculated using $i = i_k i_d/(i_k + i_d)$, Eq. 11, where i is the plotted current density, i_k is the kinetic current density from Fig. 1, and i_d is the fitted limiting current density 0.862 A cm^{-2} [8]. *Lower plot*: Plot after correction for experimental current–interruption resistance (0.22± 0.02 Ω cm^2). This perfectly reproduces the plot in Fig. 1 of [8]

above E=0.8 V vs. HE, a curved region down to about 0.72 V vs. HE, followed by a ln Tafel slope of about 2RT/F, which includes the half-wave potential region at about 0.7 V vs. HE, where α is close to 0.48. The intersection point of the low current density RT/F and high current density 2RT/F Tafel slopes is at approximately 0.78 V. The i_o values derived from this Tafel plot (corrected to the real electrochemically active electrode area) are 9.2×10^{-10} A cm^{-2} (low current density) and 2.3×10^{-6} A cm^{-2} (high current density). Because of the effect of the $q\theta_T$ term on reaction rate, these values are not particularly physically meaningful. The rate constant for the reaction is physically more important [17].

Using the Fig. 1 Tafel plot, and the second part of Eq. 11, with i_d=0.862 A cm^{-2} from [8] for the cell in question, we obtain an excellent fit to the IR-free Passalacqua et al. plot in Fig. 2. This analysis explains the difference between the IR as deconvoluted from their E–i curve and the value experimentally obtained by these authors by current interruption in the 0.3–0.4 A cm^{-2} range.

Conclusions

The agreement between the calculated expression in Fig. 2 using a Frumkin isotherm–Tafel equation approach for the Damjanovic–Brusic ORR mechanism and the Passalacqua et al. E–i curve from Fig. 1. of [8] suggest that conventional fits of PEMFC cathode performance are inaccurate because they assume a constant Tafel slope from the accessible low-current density region to throughout the range of, say, 0.6 V

and beyond. In [5], the Tafel slope value was taken to be 0.057 V per natural logarithm unit, or a slope of 1.19 RT/F at 343 K. The above model shows that i/i_k, where i is the measured current density and i_k is the kinetic or Tafel current density, under these conditions may about 88%, 68%, 41%, 22%, and 10.7% at 0.8, 0.75, 0.7, 0.65, and 0.6 V vs. HE, respectively. These might be compared with values assuming a constant Tafel slope of close to RT/F, when 88%, 57%, 19.5%, 4.2% and 0.8% are obtained at the same potentials vs. HE. It therefore seems that today's porous PEMFC electrodes behave far more effectively than is usually assumed from the viewpoint of electrocatalyst utilization at high current densities, and short of being able to greatly change the ORR mechanism, improved electrode structures allowing improved internal diffusion and higher limiting currents are required to improve their performance.

References

1. Neyerlin KC, Gu W, Jorne J, Gasteiger HA (2007) J Electrochem Soc 154:B631. doi:10.1149/1.2733987
2. Franco AA, Schott P, Jallut C, Maschke B (2006) J Electrochem Soc 153:A1053. doi:10.1149/1.2188353
3. Franco AA, Tembely M (2007) J Electrochem Soc 154:B712. doi:10.1149/1.2731040
4. Kuhn H, Wokaun A, Scherrer GG (2007) Electrochim Acta 52:2322. doi:10.1016/j.electacta.2006.03.108
5. Kim J, Lee SM, Srinivasan S, Chamberlain CE (1995) J Electrochem Soc 142:2670. doi:10.1149/1.2050072
6. Squadrito G, Maggio G, Passalacqua E, Lufrano F, Patti A (1999) J Appl Electrochem 29:1449. doi:10.1023/A:1003890219394
7. Chu D, Jiang R (1999) J Power Sources 142:226. doi:10.1016/S0378-7753(98)00263-8
8. Passalacqua E, Lufrano F, Squadrito G, Patti A, Giorgi L (2001) Electrochim Acta 46:799. doi:10.1016/S0013-4686(00)00679-4
9. Bard AJ, Faulkner LR (1980) Electrochemical methods. Wiley, New York
10. Vogel W, Lundquist J, Ross PN, Stonehart P (1975) Electrochim Acta 20:79
11. Stonehart P, Ross PN (1975) Catal Rev 12:1
12. Damjanovic A, Brusic V (1967) Electrochim Acta 12:615. doi:10.1016/0013-4686(67)85030-8
13. Marković NM Ross PN (1999) In: Wieckowski A (ed) Interfacial electrochemistry, theory, experiment, and applications. Marcel Dekker, New York, p 821
14. Stamenkovic VR, Fowler B, Mun BS, Wang G, Ross PN, Lucas CA, Marković NM (2007) Science 315:493. doi:10.1126/science.1135941
15. Stamenkovic VR, Mun BS, Arenz M, Mayrhofer JJ, Lucas CA, Wang G, Ross PN, Marković NM (2007) Nature Materials 6:241. doi:10.1038/nmat1840
16. Appleby AJ (1973) J Electrochem Soc 120:1205. doi:10.1149/1.2403662
17. Appleby AJ (2008) Electrochim Acta (to be published)
18. Appleby AJ (1974) In: Conway BE, Bockris JOM (eds) Modern aspects of electrochemistry, vol 9. Plenum, New York, p 369
19. Antoine O, Bultel Y, Durand R (2001) J Electroanal Chem 499:85. doi:10.1016/S0022-0728(00)00492-7
20. Fischer A, Jindra J, Wendt H (1998) J Appl Electrochem 28:277. doi:10.1023/A:1003259531775